TOPOLOGY OF REGULARIZED SUBMANIFOLDS IN RESTRICTED 3-BODY PROBLEM

By Ernesto A. Lacomba*

In this paper we investigate the topology of the regularized and unregularized invariant submanifolds in the restricted 3-body problem, for different values of the Jacobi constant. The results on Section 3 are essentially contained in Birkhoff [1], but the proofs and topological representations are improved, and made more geometrically clear here.

We apply some Morse theory in Section 4 to understand topological change through critical levels of the Jacobi constant. This may be the most important contribution of the paper.

In a later paper we will pursue the task of regularizing collisions in our problem, following Easton's methods and ideas [3], [2].

The reader is referred to Szebehely [6] and Pollard [4] for precise definitions and basic properties of the restricted 3-body problem.

1. Description of the problem. Techniques for calculating the topology

As it is well known, the restricted 3-body problem consists in studying the motion of a particle of zero mass (planetoid), subject to gravitational attraction from two masses of positive mass (primaries) revolving in circles about each other in the same plane [4].

The differential equations governing the motion in phase space can be written in the following form

$$(1)\qquad \begin{aligned} \dot{\xi} &= \alpha \\ \dot{\eta} &= \beta \\ \dot{\alpha} &= 2\beta + \Phi_\xi \\ \dot{\beta} &= -2\alpha + \Phi_\eta \end{aligned}$$

where $(\xi, \eta, \alpha, \beta)$ are coordinates of the 4-dimensional phase space, and

$$(2)\qquad \Phi(\xi, \eta) = \tfrac{1}{2}(\xi^2 + \eta^2) + V(\xi, \eta) + \tfrac{1}{2}\mu(1 - \mu)$$

$$(3)\qquad V(\xi, \eta) = \frac{1 - \mu}{\rho_1} + \frac{\mu}{\rho_2}$$

$$\rho_1^2 = (\xi + \mu)^2 + \eta^2,\ \rho_2^2 = (\xi - 1 + \mu)^2 + \eta^2,\ 0 < \mu < 1.$$

The *Jacobi constant* of motion is defined by

$$(4)\qquad J(\xi, \eta, \alpha, \beta) = 2\Phi(\xi, \eta) - (\alpha^2 + \beta^2),$$

its levels being invariant submanifolds, as with any constant of motion.

It is clear that $\xi = -\mu,\ \eta = 0$ or $\xi = 1 - \mu,\ \eta = 0$ represent singularities

* Acknowledgment. The author is grateful to A. Verjovsky for some helpful hints.

of the functions (2), (3) and the differential equations (1). They correspond to collisions of the zero mass particle with either of the primaries.

From (4) we easily see that if the Jacobi constant has a value C, then $\Phi(\xi, \eta) \geqslant C/2$ in order for any motion to take place. This condition does not represent any restriction on the projection to configuration space of the corresponding level submanifold, unless $C \geqslant 3$ [4]. Indeed, equation (4) says that when $J = C$ we have

$$\alpha^2 + \beta^2 = 2\Phi(\xi, \eta) - C \tag{5}$$

so that the invariant submanifold is a pinched cell bundle over $\Phi(\xi, \eta) \geqslant C/2$ in $\boldsymbol{R}^2$, in Smale's terminology, the pinching occurring over the boundary $\Phi(\xi, \eta) = C/2$.

This boundary is called a *zero velocity curve* for the value C of the Jacobi constant, due to the fact that according to (5) the only allowed velocity for those configuration points is zero.

A first step towards finding the topology of the invariant submanifolds is to find the topology of the zero velocity curves, which is a more or less standard result known from numerical methods [6], [4]. In the following figures we describe the zero velocity curves, and the regions $\Phi \geqslant C/2$ for progressively decreasing values of C. The said regions are projections of the Jacobi levels into configuration space:

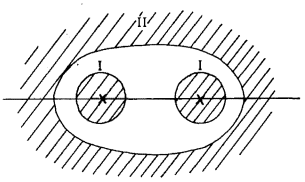

Fig. 1

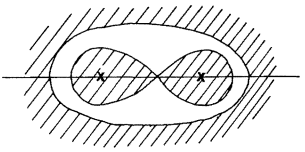

Fig. 2

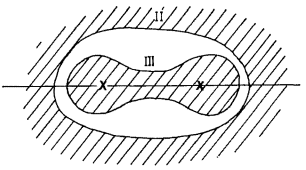

Fig. 3

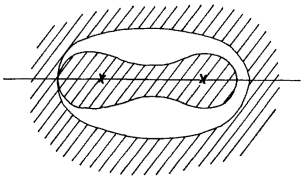

Fig. 4

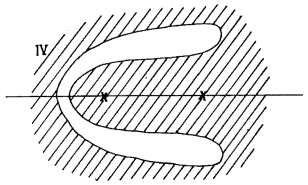

Fig. 5

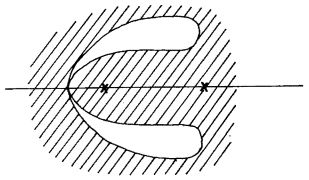

Fig. 6

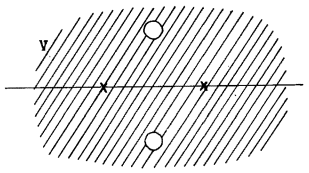

Fig. 7

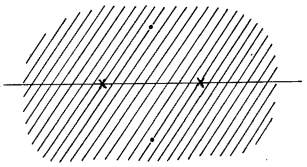

Fig. 8

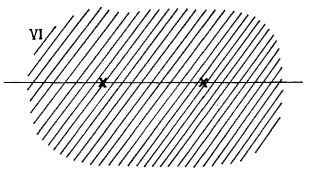

Fig. 9

We will restrict ourselves to computing the topology for Figures 1, 3, 5, 7 and 9, corresponding to noncritical levels of J. It will be enough to consider the pinched cell bundle over the six different regions numbered I, II, III, IV, V and VI in the figures.

Notice that Fig. 8 corresponds exactly to the case $C = 3$.

Up to here we have just been talking about unregularized Jacobi levels, where the 2 collision points are eliminated ("crosses" in the figures above) when constructing the pinched bundle. Regarding the regularized levels, it will be enough to adjoin two solid tori, conveniently identifying their boundaries in each of the two "holes" left. This will be accomplished by using Levi-Civita regularized coordinates for the problem [6].

2. Unregularized submanifolds

We will get the topology of the unregularized submanifolds in such a way that it will be easy to see how they transform in regularizing.

It will be convenient to excise sufficiently small closed balls centered at the collision points instead of simply eliminating the points and (since the zero velocity curves are compact) to cut each unbounded region in the plane by a sufficiently big open ball centered at the origin. This procedure does not change the resulting topology at all.

Case I).—We have to construct the pinched cell bundle over the following region

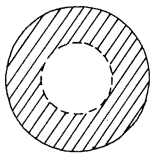

We have to pass a circle S^1 through each point of the region, except at the boundary (zero velocity curve), where it corresponds to just one point. We might think that the radius of those circles approaches zero as we move towards the boundary, so that we may construct them as contained in the orthogonal radial plane through each point and with center at the zero velocity curve. We get an open solid torus whose boundary corresponds to points approaching collisions, the central circle representing the zero velocity curve:

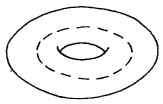

Fig. 10

Case II).—In this case the region is as follows.

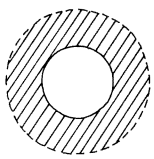

The topology is as in case I, the only difference being that points approaching the boundary of the solid torus here, are the ones whose distance to the origin goes to ∞ in the configuration plane.

Case III).—The region here is of the form

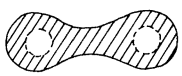

To find the topology of the pinched cell bundle, we cut through a segment joining the two holes and proceed as in Case I, above, getting

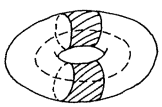

This is a solid torus where the two shaded rings at the boundary must be correspondingly identified, since they correspond to the cutting segment.

If we think in making very thin one of the two nonshaded portions of the torus

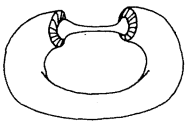

it is not hard to see by identifying that the result is a torus minus a smaller torus, as follows,

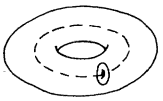

Fig. 11

where the dotted line corresponds to the zero velocity curve, the two tori corresponding to each one of the collisions.

Notice that the situation is symmetrical in the sense that we might as well have interchanged roles of the boundary tori during the identification taking either one outside in, and the other inside out.

Case IV).—

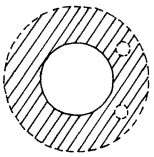

This case is almost like case III, except that now the holes corresponding to collisions generate two tori around the zero velocity curve:

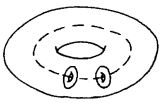

Fig. 12

Case V).—Here we have a region of the following form,

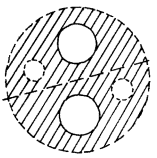

where we found convenient to cut it into half by the dotted line, and to paste it back after making the constructions.

Identifications of each half to give the pinched cell bundle provides two

copies of the following solid torus, which should be glued each other at the shaded region on the boundary:

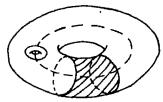

Fig. 13

As usual, the central circles represent the zero velocity curves, while the inner tori approach collisions.

To express the topology in a more convenient form, we start by considering the following circle

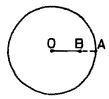

It is clear that from this figure we may open the slot OB and deform so as to get an annulus,

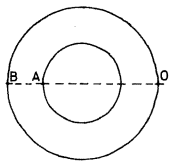

where the inner circle represents the original circle, and points on the outer circle must be identified symmetrically with respect to OB, to recover the segment. This transformation can actually be carried out in the plane without going to 3 dimensions, if we start by cutting OA, deforming, and gluing back AB.

Our last remark permits to generalize the procedure so as to apply it to one of the two copies of the solid torus, above: Assume that the solid torus is generated by rotating the given circle about the axis, as indicated below. The line segment OA generates a cut on the torus, which will not affect the interior curve and torus, since we are free to move them inside.

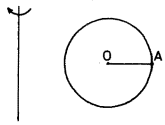

Cutting and pasting as above gives a thick torus with certain points of the outer boundary identified, while the inner boundary is topologically the same as the original boundary, with its shaded region.

Now we take the untouched copy of the solid tori and put it in the inside, identifying shaded regions. The result is the following figure with boundary

identified:

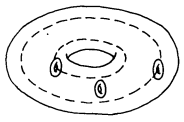

Fig. 14

The two tori knotted with the zero velocity curves correspond to collisions, while the unknotted torus represents points getting away from the origin. The identification on the outer torus can be described as follows: trace two different parallels on it, and then the rest of the points must be identified by pairs, so as to give an annulus where the inner and outer circles correspond to the chosen parallels.

Case VI).—This case is very simple, since the region goes as follows,

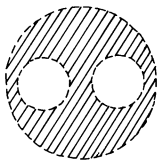

so that we get a solid torus minus two concentric tori (in this case there is no pinching at all).

3. Regularized submanifolds

We will start by describing Levi-Civita regularized coordinates [6], [1]. These equations regularize either one of the two collision singularities, and since they are symmetrical in this sense and we are interested only in topological considerations, it will be enough to regularize at the point $\xi = 1 - \mu$, $\eta = 0$.

By using complex numbers and letting $z = \xi + i\eta$, the system of differential equations (1) can be written in the form

$$\ddot{z} + 2i\dot{z} = \operatorname{grad}_z U \tag{6}$$

where

$$U = \tfrac{1}{2}[(1-\mu)\rho_1^2 + \mu\rho_2^2] + \frac{1-\mu}{\rho_1} + \frac{\mu}{\rho_2} - \frac{C}{2} \tag{7}$$

and grad_z indicates gradient with respect to the variables ξ, η, keeping fixed the Jacobi constant C.

Using (4), it is not hard to prove that to fix the Jacobi constant implies that the following equation, which is essentially (5), is satisfied on Jacobi levels:

$$|\dot{z}|^2 = 2U \tag{8}$$

Levi-Civita regularizing transformation at $z = (1 - \mu)$ is defined by the fol-

lowing equations

$$z = f(w) = w^2 + 1 - \mu \tag{9}$$

$$\frac{dt}{d\tau} = \left|\frac{df}{dw}\right|^2 = 4|w|^2 \tag{9'}$$

which transforms (6) into the form (prime denotes derivates with respect to τ):

$$w'' + 8i|w|^2 w' = \text{grad}_w (4|w|^2 U) \tag{10}$$

Notice that the regularizing transformation is made on Jacobi levels, since the right member of (10) actually does depend on C, though that was not true of (6).

Equations (7) and (8) become now

$$4|w|^2 U = 2\left[(1-\mu)|w^2+1|^2 + \mu|w|^4 + 2\frac{1-\mu}{|w^2+1|} - 2C\right]|w|^2 + 4\mu, \tag{11}$$

$$|w'|^2 = 8|w|^2 U \tag{12}$$

We can easily see that the regularizing equations (9), (9') induce a transformation of phase space by the following map

$$F(w, w') = \left(1 - \mu + w^2, \frac{ww'}{2|w|^2}\right) = (z, \dot{z}) \tag{13}$$

To get the topology of the integral manifolds in regularized coordinates we also need to construct pinched cell bundles over the corresponding regions in w-plane, according to (12). The difference now is that we have to simulate the return to the original z-coordinates by identifying points symmetrical to the origin in (w, w')-phase space, since the map F is two to one, except at the origin, as we can check $F(-w, -w') = F(w, w')$.

We will now examine the regularized situation for the six cases considered in Section 2. Since a region in z-plane of either case I), or I'): a small open ball around the singularity $z = 1 - \mu$, are topologically preserved by transformation (9), it will be enough to study these two cases by identifying pinched cell bundles constructed as in the unregularized situation. We then apply I' (extending its result to the other collision $z = -\mu$, since the situation is similar) to cases III to VI, so to see how topology changes when regularizing.

Case II is unchanged under regularization, since the region in this case does not contain any collision.

Case I).—We claim that the regularized submanifold here is projective 3-space, as in the negative energy levels of the plane 2-body problem [2].

Indeed, we first see that the pinched cell bundle over the following region is S^3(3-sphere):

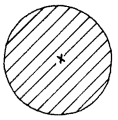

Since pinched cell bundles over diffeomorphic regions in the plane are diffeomorphic, we may assume that our region is $D: |w|^2 \leqslant 1$. One possible way of getting the pinched bundle is by taking the "circle" $|w'|^2 = 1 - |w|^2$ for any fixed w in D. The equation $|w|^2 + |w'|^2 = 1$ clearly represents S^3 in phase space. Identifying antipodal points gives P^3, as asserted.

Notice that in this case we actually got the pinched cell bundle as a smooth manifold. In general, it can be smoothed out at the boundary [5], so that it becomes not only homeomorphic, but diffeomorphic to the noncritical levels of C.

If we represent P^3 as the following ball with antipodal points at the boundary identified, the interior dotted circle corresponds to the zero velocity curve, while the circle we get after identifying endpoints in the vertical line corresponds to collisions:

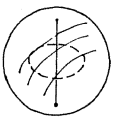

Case I′).—We consider now a small open ball around the collision:

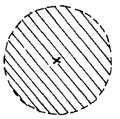

We claim that the corresponding regularized region is an open solid torus.

As above, it will be enough to consider the set $\{(w, w'): |w| < 1, |w'| = 1\}$ and identify symmetrical points. If we parametrize w' by an angle $-\Pi \leqslant \theta \leqslant \Pi$, our set can be represented by the following open solid cylinder with top and bottom identified

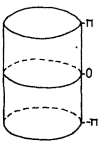

The identification $(w, w') \leftrightarrow (-w, -w')$ now becomes $(w, \theta) \leftrightarrow (-w, \theta - \Pi)$ for $0 \leqslant \theta \leqslant \Pi$, so that the lower part of the cylinder is superfluous under identification. We are left with $\{w: |w| < 1\} \times [0, \Pi]$ with top and bottom identified according to $(w, 0) \leftrightarrow (-w, \Pi)$. This gives a solid torus twisted by an angle Π before identifying.

There is a standard procedure [2] to identify the boundary of two solid tori by properly twisting, so as to give P^3. If we apply it to the torus in case I′ and the torus in the unregularized case I of Section 2, we get the result of case I, above. In this sense the twisted torus of case I′ can be seen as a subset of P^3,

by the cylinder of the following figure with proper identifications (collisions are represented by the central circle, as before):

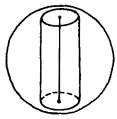

This kind of identifications of tori will be central to the determination of regularized submanifolds in the other cases.

We also remark that by conveniently cutting and pasting it is easy to see that a solid sphere minus a small solid torus (drilled in it) is topologically equivalent to a solid torus minus a small solid sphere inverting the two boundary components. Similarly, a solid torus minus a smaller solid torus is equivalent to another one where its two boundary components have changed roles. By working freely with these inversions and having in mind the identification of two tori to give P^3, it is easy to see that any torus boundary corresponding to a collision is transformed by regularization into a sphere S^2 where antipodal points are identified. The passing from case I in Section 2 to the regularized case I, above is a particular case of this situation, since P^3 is being represented as a closed 3-ball with its boundary S^2 identified by antipodal points.

In the following figures all the boundary components S^2 appearing will be understood as antipodally identified.

Case III).—Here the result from the same unregularized case in Section 2 becomes as shown by the following figure, where dotted lines represent zero velocity curve, and the others knotted around represent collision states, as usual.

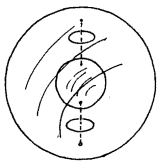

Case IV).—Working again with the unregularized submanifold corresponding to the same case, we get a description of the regularized submanifold given by either one of the following equivalent figures.

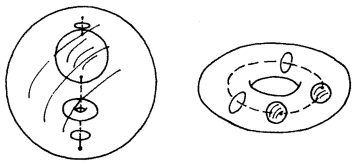

Case V).—We get the following figure, where each zero velocity curve reaches

both copies of S^2 in different points, and the outer boundary must be identified as described in Section 2 for the unregularized situation.

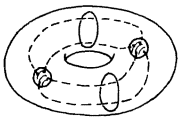

Case VI).—We get the following figure, with the two knotted circles corresponding to collision.

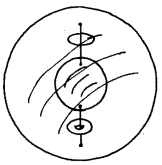

4. Passing through critical levels by Morse Theory

We conclude this paper by rapidly describing the effect on the topology of passing through critical levels of the function J.

The critical points of J in phase space are exactly the critical points of system (1), and these are the critical points of Φ in the configuration plane, taken with zero velocity. It is well known [4], [6] that Φ has exactly five critical points. The first three are called *Euler points* and are collinear with the primaries, located in each one of the three line portions defined by the primaries. The other two are named *Lagrange points* and are situated in each of the two vertices of equilateral triangles with 2 vertices at the primaries.

By straightforward computation we find that the 5 critical points for J are nondegenerate, and they have indices 3 for the Euler points, and 2 for the Lagrange points. So, we can use Morse Theory to describe the topology change when the values of J pass through critical levels.

We will refer to Figures 1 to 9 and regions I to VI of Section 1 very often. The critical points of J occur exactly when the zero velocity curves touch at the Euler and Lagrange points (Figs. 2, 4, 6, 8). The reason for this is that the critical points of J and Φ are essentially the same, as described above.

Since the situation is a local one, it will be enough to operate on the unregularized Jacobi levels of Section 2, so that references will be made also to Figures 10 to 14 of the said section.

We will consider the process of attaching one 4-cell D^4 (a topological closed ball in 4-space) for each nondegenerate critical point when passing critical levels, as described by Theorem 5.1 in [7]. The only reinterpretation is that we will apply it for decreasing values of C, since Figs. 1 to 9 were drawn that way, with Fig. 8 corresponding to $C = 3$.

Recall that dimension of phase space is 4. The version of the theorem for the Euler points reads as follows.

PROPOSITION 1. *For each of the Euler points where* $n = 4$ *and the index is* $r = 3$, *the passing through a critical level from a value slightly greater to a slightly smaller is accomplished by attaching a 4-cell as neighborhood of the critical point, whose boundary is a union of 3 sets diffeomorphically described as* $A = D^3 \times S^0$, $B = S^2 \times D^1$, $E = S^2 \times S^0 \times I$ (D^k *is k-cell, or closed ball in k-space*). *The sets A and B are disjoint and respectively contained in each of the two regular levels of C. The portion E serves as a link between A and B, identifying points* $(p, q) \in \partial D^3 \times S^0 \subset A$ *with* $(p, q, 0) \in E$, *and points* $(p, q) \in S^2 \times \partial D^1$ *with* $(p, q, 1) \in E$. *If* D^4 *is removed, the portions of the Jacobi levels left are isotopic.*

Fig. 2).—We need to take two copies of Fig. 10, and excise one interior closed ball containing the zero velocity curve in each (this gives A). In place of the excised closed balls we must glue correspondingly each of the two boundary components of the thick sphere $S^2 \times D^1 = B$. This can be accomplished by first introducing the thick sphere into one of the torus with excised balls, operation after which this remains topologically the same:

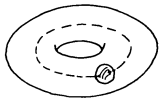

Finally, we take the other copy, inverting as in Section 3 to get the sphere outside and the torus inside, introducing them into above figure identifying bounding spheres. The result is clearly Fig. 11, as asserted.

Fig. 4).—In this case Prop. 1 gives the same description as above, since we are dealing with another Euler point. We take a copy of Fig. 10 and a copy of Fig. 11, and excise one closed ball containing a zero velocity curve in each. The result gives an excised small torus linked with the curve in Fig. 11. This is Fig. 12.

Fig. 6).—This is the third Euler point, so we apply Prop. 1 again to Figure 12. The single zero velocity curve in this figure is broken into two in passing the critical level, so that we have to excise the two closed 3-balls over said curve, as shown by the following figure

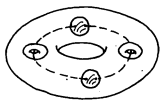

In order to get two curves from the original one, we cut this figure by a plane passing by the "centers" of the excised balls and transversal to the curve. We get two copies of the following figure, where the shaded region on each must be identified together:

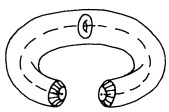

We now identify together each of the 2-cells (half spheres) according to Proposition 1, and so that the 2 points on the zero velocity curve agree. We get two copies of Fig. 13, where the shaded regions must be identified as described below that figure. This gives Fig. 14, as asserted.

Fig. 8).—Theorem 5.1 in [7] now states the following.

PROPOSITION 2.—*For each of the Lagrange points where* $n = 4$ *and the index is* $r = 2$, *the passing through a critical level from a value slightly greater to a slightly smaller is accomplished by attaching* 4*-cells* D^4 *as neighborhoods of each critical point, whose boundary is a union of the* 3 *sets diffeomorphically* $A = D^2 \times S^1$, $B = S^1 \times D^2$ *and* $E = S^1 \times S^1 \times I$ *with* A *and* B *disjoint and contained respectively in each of the two levels of* C. *The set* E *is a link between* A *and* B, *identifying points* $(p, q) \in \partial D^2 \times S^1 \subset A$ *with* $(p, q, 0) \in E$, *and* $(p, q) \in S^1 \times \partial D^2 \subset B$ *with* $(p, q, 1) \in E$.

The idea here is that at each critical point we must cut a solid torus, and in the bounding torus left identify another solid torus where the role of meridians and parallels is interchanged.

We have to start with Fig. 14, and since both zero velocity curves are collapsed at the same time at the 2 Lagrange points, the operation must interest both curves, with one solid torus for each curve.

Recalling that the boundary of Fig. 14 must be identified in the way described with it, we may think of the curves as the inner and outer parallels with the same reflective identifications at the boundary of the following figure:

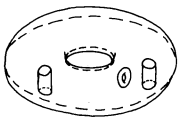

Cutting two small solid tori with center line the curves, and attaching in their old boundaries solid tori with center line orthogonal to those, is equivalent to take the following 3 figures

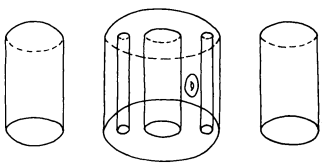

with top and bottom identified correspondingly in each one. The boundaries of each simple solid torus must be identified respectively with each one of the boundary components of the other figure, in the order shown above. We may first locate one solid torus in the hole of the figure and identify top and bottom, getting a torus without two concentric tori and without a small torus unlinked to either.

The outer boundary must be identified to the outer boundary of the simple torus left. Making a toral inversion as in Section 3, this is equivalent to filling

the small unknotted hole with the torus. We get a torus minus two concentric tori as in case VI of Section 2.

Remark.—In the exceptional case $\mu = \frac{1}{2}$ the two zero velocity curves touch symmetrically in two Euler points, and so Figures 5 and 6 do not happen. Passing through critical level from Fig. 3 to Fig. 7 can be described by performing the operation for Figs. 4 and 6 at the same time.

UNIVERSIDAD AUTONOMA METROPOLITANA
UNIDAD IZTAPALAPA, MEXICO, D.F.

REFERENCES

[1] G. D. BIRKHOFF, *The restricted problem of three bodies*, Rend. Circ. Mat. Palermo **39** (1915), 1–70.
[2] R. EASTON, *Regularization of vector fields by surgery*, J. Differential Equations **10** (1971), 92–9.
[3] R. EASTON, *The topology of the regularized integral surfaces of the 3-body problem*, J. Differential Equations **12** (1972), 361–84.
[4] H. POLLARD, Mathematical Introduction to Celestial Mechanics, N. Jersey, Prentice Hall, 1966.
[5] S. SMALE, *Topology & mechanics* II, Invent. Math. **11** (1970), 45–64.
[6] V. G. SZEBEHELY, Theory of Orbits, New York, Academic Press, 1967.
[7] A. WALLACE, Differential Topology, First Steps, New York, Benjamin, 1968.